ARTICLE

BIOTECHNOLOGY and BIOENGINEERING

Characterization of a Gastrointestinal Tract Microscale Cell Culture Analog Used to Predict Drug Toxicity

Gretchen J. Mahler,[1] Mandy B. Esch,[2] Raymond P. Glahn,[3] Michael L. Shuler[2]

[1]School of Chemical and Biomolecular Engineering, Cornell University, Ithaca, New York

[2]Department of Biomedical Engineering, Cornell University, 115 Weill Hall, Ithaca, New York 14853; telephone: 1-607-255-7577; fax: 1-607-255-1136; e-mail: mls50@cornell.edu

[3]Plant, Soil and Nutrition Laboratory, Agricultural Research Services, U.S. Department of Agriculture, Tower Road, Ithaca, New York 14853

Received 18 December 2008; revision received 12 March 2009; accepted 6 April 2009

Published online 13 April 2009 in Wiley InterScience (www.interscience.wiley.com). DOI 10.1002/bit.22366

ABSTRACT: The lining of the gastrointestinal (GI) tract is the largest surface exposed to the external environment in the human body. One of the main functions of the small intestine is absorption, and intestinal absorption is a route used by essential nutrients, chemicals, and pharmaceuticals to enter the systemic circulation. Understanding the effects of digestion on a drug or chemical, how compounds interact with and are absorbed through the small intestinal epithelium, and how these compounds affect the rest of the body is critical for toxicological evaluation. Our goal is to create physiologically realistic in vitro models of the human GI tract that provide rapid, inexpensive, and accurate predictions of the body's response to orally delivered drugs and chemicals. Our group has developed an in vitro microscale cell culture analog (μCCA) of the GI tract that includes digestion, a mucus layer, and physiologically realistic cell populations. The GI tract μCCA, coupled with a multichamber silicon μCCA representing the systemic circulation, is described and challenged with acetaminophen. Proof of concept experiments showed that acetaminophen passes through and is metabolized by the in vitro intestinal epithelium and is further metabolized by liver cells, resulting in liver cell toxicity in a dose-dependent manner. The μCCA response is also consistent with in vivo measurements in mice. The system should be broadly useful for studies on orally delivered drugs or ingestion of chemicals with potential toxicity.

Correspondence to: M.L. Shuler

Contract grant sponsor: New York State Office of Science, Technology and Academic Research (NYSTAR) Program

Contract grant sponsor: National Science Foundation

Contract grant number: ECS-9876771, ECS-0335765

Contract grant sponsor: Army Corps of Engineers

Contract grant number: W9132T-07-2-0010

Contract grant sponsor: U.S. Department of Agriculture

Additional Supporting Information may be found in the online version of this article.

Biotechnol. Bioeng. 2009;104: 193–205.

KEYWORDS: cell culture analog; GI tract; acetaminophen; toxicity; drug testing; in vitro

Introduction

The process of developing a new drug includes pre-clinical assessments such as biochemical and cellular assays and animal toxicity testing before final validation in human clinical trials. Recently, the majority of drug candidates have failed in phase III clinical trials, highlighting the need for a better method to accurately assesses the absorption, distribution, metabolism, elimination, and toxicity (ADMET) of drug candidates early in the development process (Agres, 2005). Two preliminary methods commonly used to determine the toxicological and pharmacological profiles of potential drugs are in vitro cell cultures and animal models. Single cell type, monolayer cell cultures cannot measure the systemic changes caused by the compound of interest and its metabolites, and animal experiments can take months to complete, require large amounts of product, and the majority of drugs shown to be safe in animals fail in human clinical trials (Sankar, 2005).

This work describes an in vitro cell culture analog (CCA) that may be able to better predict human response to oral drug exposure. A CCA is a physical representation of a physiologically based pharmacokinetic (PBPK) model. A PBPK model, which describes an organism as a set of

interconnected tissue or organ compartments that are based on vasculature structure, is designed to calculate the time-dependent distribution of a chemical or drug in various tissues (Brown et al., 1997). The CCA devices consist of channels and chambers arranged and sized to mimic the residence time and flow distribution of the corresponding PBPK model. Where the PBPK model mathematically specifies an organ, for example, the CCA has an actual chamber holding a cell type that mimics the key features of that organ, while the CCA fluidics are designed to mimic the essential features of the circulatory system with re-circulating culture medium acting as a blood surrogate. The goal of a CCA is to create an in vitro system that can replicate some of the cell–cell interactions (i.e., interactions through soluble proteins and metabolites) in humans or animals not easily studied in vivo or in silico and to apply these observations to toxicology studies.

A three-chamber (lung, liver, and other tissues) microscale cell culture analog (μCCA) was previously developed using tools from the semiconductor industry (Sin et al., 2004). The μCCA consists of etched cell compartments and channels on a 2.5 cm × 2.5 cm silicon chip with culture medium re-circulated through the chip using a peristaltic pump. A four-chamber (lung, liver, fat, and other tissues) μCCA was used to demonstrate the effects of naphthalene on various tissues (Viravaidya et al., 2004). In this study, naphthalene added to the culture medium was converted to reactive metabolites in the liver compartment, and when these metabolites circulated to the lung compartment the result was lung cell death. Later experiments using adipocyte-like cells in the fat chamber showed how fat could modify the response (Viravaidya and Shuler, 2004). These experiments demonstrated that the μCCA can re-create the known effects of a toxic chemical. More recently, a μCCA has been used to evaluate drug mixtures for potential multi-drug-resistant cancer treatments (Tatosian and Shuler, 2009). The microscale size of the device allows for near in vivo organ residence times, fluid to tissue ratios, and cellular shear stress values. The small size also decreases manufacturing costs, reagent or sample amounts, and space needed.

In previous work with the μCCAs, drug was added directly to the circulating culture medium, which mimics intravenous administration of a compound. Oral delivery, however, is the preferred route of pharmaceutical administration due to relatively low medical costs and relatively high patient comfort, compliance, and convenience; but the intestinal wall acts as a biological barrier that both limits the uptake of and biotransforms drugs (Lampen et al., 1998; Lee, 2002). Biotransformation occurs during transcellular absorption when pharmaceuticals come in contact with phase I and phase II enzymes (Doherty and Charman, 2002). The most notable phase I enzymes belong to the cytochrome P450 superfamily which oxidize compounds, especially chemicals or drugs that are hydrophobic and relatively insoluble, to form a reactive intermediate (Rang et al., 1999). The reactive intermediate is then susceptible to conjugation by a phase II enzymes such as UDP-glucuronyltransferase, sulfotransferase, or glutathione-*S*-transferase (Doherty and Charman, 2002). The resulting conjugate is usually pharmacologically inactive and less lipid soluble than its precursor, allowing the conjugate to be excreted in bile or urine (Rang et al., 1999).

The membrane lining the small intestine is composed of two main cell types: enterocyte and goblet. Absorptive enterocytes make up about 90% of the cell population, display very tight intracellular junctions, are covered in surface area enhancing microvilli, and allow the passage of small molecules by one or more of four different routes: passive transcellular (through the cell), passive paracellular (between cells), active (energy-dependent) carrier-mediated, and transcytosis (transport across the epithelium with uptake into coated vesicles) (Artursson et al., 2001; Forstner and Forstner, 1994). The ratio of goblet cells ranges from 10% in the small intestine to 24% in the distal colon (Forstner and Forstner, 1994). Goblet cells secrete mucus that forms a coating over the epithelial layer. In the duodenum, where most absorption takes place, the firmly adherent mucus layer is approximately 15 μM thick (Atuma et al., 2001; Newton et al., 2000). Any material that is absorbed through the intestine into the blood stream must first diffuse across the mucus layer, the epithelial cells lining the intestine, the lamina propria, and the endothelial cells that line the capillaries, but the epithelial cell layer has been shown to be the rate-limiting step (Audus et al., 1990). Wikman et al. (1993) have shown that the mucus layer produced by HT29-H cells presents a significant barrier to the absorption of the lipophilic drug testosterone, however, which suggests that the mucus layer may be an important consideration when estimating drug absorption in vitro.

Blood that reaches the liver from the portal vein is derived from splanchnic circulation, which includes blood flow from the stomach, small intestine, large intestine, pancreas, and spleen (Brown et al., 1997). Once a drug has absorbed across the small intestine and reached the blood within the surrounding capillary network, it is immediately delivered to the liver, which is a phenomenon called first pass metabolism. The result of first pass metabolism can be an extensively reduced concentration of bioavailable, active drug due to phase I and phase II liver metabolism.

There have been several in vitro models developed that mimic first pass metabolism. Two static models by Choi et al. (2004b) and Lau et al. (2004) used Caco-2 cells cultured on a permeable membrane with HepG2 liver cells or primary human hepatocytes cultured in the bottom of the same well as the Caco-2 cells. Both of these systems lack re-circulation and use a relatively large volume of culture medium and the compound being examined when compared with the μCCA system. Brand et al. (2000) developed an in vitro diffusion/perfusion system which studied drug transport across Caco-2 cells cultured on a semipermeable membrane and downstream response by HepG2 liver cells in a separate cell culture compartment.

This system required two syringe pumps and computer control, ran at a flow rate of 4 mL/h without re-circulation, and only one experiment could be performed at a time. Choi et al. (2004a) developed a physiologically based, multi-compartment, in vitro perfusion system with re-circulation that could be used to study intestinal drug absorption and first pass metabolism by the liver. The large volume of culture medium used in this system prevents physiologically realistic residence times, in vivo-like liquid/cell ratios, and requires a large amount of the compound being studied.

The purpose of this work is to connect an independent gastrointestinal (GI) tract μCCA to a multi-chamber systemic μCCA, which may provide a superior in vitro method for testing the ADMET of orally administered pharmaceuticals. Acetaminophen (APAP) was used as a model drug because APAP toxicity is closely linked to its metabolism by GI and liver cells. Therapeutic APAP doses are primarily metabolized by phase II conjugation with sulfate and glucuronide, but approximately 5–10% is oxidized by cytochrome P450 (CYP) 1A2, 2E1, or 3A4 to *N*-acetyl-*p*-benzoquinone (NAPQI), a toxic, electrophilic metabolite (Bessems and Vermeulen, 2001; Corcoran et al., 1980; Patten et al., 1993). NAPQI is detoxified by conjugation with glutathione via glutathione-*S*-transferase and excreted in urine or bile (Mitchell et al., 1973). Large doses of APAP that overwhelm the sulfation and glucuronidation pathways and/or the induction of CYP enzymes with drugs such as ethanol can result in high levels of NAPQI (Bessems and Vermeulen, 2001). Excessive levels of NAPQI deplete glutathione levels and the accumulated NAPQI electrophilically attacks proteins in nearby cells, causing cell death (Qiu et al., 1998).

Work using an earlier version of the systemic and GI tract μCCAs with APAP as a model drug has been described (McAuliffe et al., 2008). We have further developed this system by adding more physiologically realistic intestinal cell populations that form a mucus layer and a digestion mimic. The revised μCCA system uses a five-compartment model; liver, kidney, fat, and bone marrow compartments were etched into a silicon systemic μCCA and the GI tract μCCA is a independent device fabricated from plexiglass with apical and basolateral chambers separated by intestinal cells on a microporous membrane. Two of the chambers (liver and GI) contain cells, while the other compartments mimic the distribution of fluid in well-perfused or poorly perfused tissues. APAP was used to test the hypothesis that drug passes through and is metabolized by the intestinal epithelial monolayer in the GI tract μCCA, and APAP and metabolites circulate to the liver compartment on the systemic μCCA where the drug is further metabolized resulting in glutathione depletion and liver cell death.

The HepG2/C3A cell line, which has detectable CYP1A and 2E1, UDP-glucuronyltransferase, sulfotransferase, and glutathione-*S*-transferase activity, was used to model the liver (Hewitt and Hewitt, 2004). Co-cultures of the Caco-2 and HT29-MTX cell lines were used to mimic the intestinal cell population. Caco-2 cells, which develop tight junctions, possess microvilli, can transport small molecules by all four major transport routes, and express many phase I and phase II enzymes; are used in this model to mimic absorptive enterocytes (Artursson and Karlsson, 1991; Baranczykkuzma et al., 1991; Borlak and Zwadlo, 2003; Prueksaritanont et al., 1996). HT29-MTX cells were used to mimic goblet cells. HT29-MTX cells are a subpopulation of HT29 human colonic adenocarcinoma cells selected for resistance to methotrexate (MTX) that consist exclusively of differentiated, mucus-secreting, goblet-like cells that retain their differentiated phenotype after reversion to MTX-free medium (Lesuffleur et al., 1990). Co-cultures of Caco-2 and HT29-MTX represent the two major cell types found in the small intestinal epithelium, form tight junctions, and possess mucus layer that is 2–10 μm thick (Hilgendorf et al., 2000; Mahler et al., 2008; Walter et al., 1996). Our previous work with in vitro digestion and co-cultures of Caco-2 and HT29-MTX cells used to predict iron bioavailability showed that cell monolayers with the physiologically realistic ratios of 90:10 and 75:25 (Caco-2:HT29-MTX) were responsive to changes in sample iron bioavailability and had a mucus layer that completely covered the cell monolayer (Mahler et al., 2008). In this work, a ratio of 75:25 (Caco-2:HT29-MTX) was used.

Materials and Methods

Cell Culture

The Caco-2 (human colon carcinoma), HepG2/C3A (human hepatocellular carcinoma) cell lines were obtained from the American Type Culture Collection (Manassas, VA). The HT29-MTX cell line was kindly provided by Dr. Thécla Lesuffleur of INSERM U560 in Lille, France (Lesuffleur et al., 1990). Caco-2 cells were received at passage 17 and used in experiments at passage 30–35. HT29-MTX cells were received at passage 11 and used in experiments at passage 14–19, and HepG2/C3A cells were received at an unknown passage and used in experiments at passage $n+10$ to $n+20$. Caco-2 and HT29-MTX were grown in Dulbecco's modified Eagle medium (DMEM; Invitrogen, Grand Island, NY) containing 4 mM Glutamax, 4.5 g/L glucose, and 10% heat inactivated FBS (Invitrogen). HepG2/C3A cells were maintained in minimal essential medium (MEM; Invitrogen) with 1.0 mM sodium pyruvate and 10% FBS (Invitrogen). MEM used in all experiments contained 1.0 mM sodium pyruvate and 10% FBS.

μCCA Fabrication

The systemic μCCA was fabricated at the Cornell Nanofabrication Facility using standard photolithography and etching techniques that have been described previously (Sin et al., 2004). The chip pattern was first designed on CAD (Cadence, Fishkill, NY), and the pattern was converted

onto a chrome-coated glass mask via the 3600F optical pattern generator (D.W. Mann/GCA Corp., Burlington, MA). Two masks were required for the two layers of fabrication, a 30 μm etch and a 100 μm etch.

Silicon dioxide layers (93 nm thick) were grown on silicon ⟨1 0 0⟩ wafers (Silicon Quest, Santa Clara, CA) at 1,100°C under 8 L/min O_2 flow and 0.24 L/min HCl flow in a furnace tube. The wafers were covered with Shipley 1813 photoresist (Shipley Company, Marlborough, MA) at a spin speed of 3,000 rpm resulting in a 1.3-μm thick layer of photoresist. The pattern was transferred to the resist via a 4-s UV light (405 nm) exposure on a contact aligner (AB-M HTG 3HR Contact Proximity Aligner, San Jose, CA) and subsequent development for 2 min. Residual resist was removed using oxygen plasma for 30 s and the silicon dioxide layer was etched using a CHF_3/O_2 plasma for 15 min at 40 mTorr, 50 sccm CHF_3, 2 sccm O_2, and 40% RF power. The channels were then etched with a UNAXIS 770 plasma etcher (Unaxis USA, Inc., St. Petersburg, FL) using a DRIE process until the depth measured 30 μm. The resist and oxide were removed using Remover 1165 (Shipley Company) and buffered oxide etch (6:1) for 5 min, respectively. New silicon dioxide layers were grown using dry oxidation as described above. The wafers were then coated with Shipley STR 1045 photoresist at 1,000 rpm and baked at 95°C, ramped up stepwise from 25°C in 8 min. The resist thickness was relatively non-uniform owing to the already etched channels, but in general measured between 10 and 12 μm. The second mask pattern was transferred to the wafer with UV light for 20 s using the HTG contact aligner and developed for 6 min. Residual resist was removed using the same process described above. The second set of channels was etched using the DRIE process until the etch depth measured 100 μm. The resist was stripped with Remover 1165 and the channel depth checked again. If needed, the channels were etched for one or two more cycles to obtain an exact etch depth. The oxide layer served as an additional masking layer, since the resist is non-uniform and measurement of the etch depth with resist may vary depending on the position of measurement. Figure 1A shows a photograph of the systemic μCCA.

The GI tract μCCA was fabricated from 1/2 in. thick plexiglass (McMaster-Carr, New Brunswick, NJ) by Glenn Swan (School of Chemical and Biomolecular Engineering, Cornell University). The top and bottom pieces were machined to fit a 12-mm diameter Snapwell™ insert (Corning Life Sciences, Corning, NY). Identical chambers were etched into the top and bottom pieces on the surface that contacted the membrane holding intestinal epithelial cells. The chambers were 0.8 mm deep, 2.4 mm in diameter on the side facing the cell membrane, and 0.8 mm in diameter where the inlet and outlet holes were drilled. The top and bottom pieces had two-step inlet and outlet channels drilled with a diameter of 740 μm (drill size number 69; Small Parts, Inc., Miami Lakes, FL) for the top half of the channel and 610 μm (drill size number 73; Small Parts, Inc.) for the bottom half of the channel. Figure 2 shows the GI tract μCCA device.

μCCA Assembly

Polycarbonate, 0.4 μm pore size, 12 mm diameter Snapwell membranes were coated with 200 μL of Type I collagen dissolved in 0.02 M acetic acid at a concentration of 50 μg/mL for 1 h and then washed with an equal volume of PBS. Caco-2 and HT29-MTX cells at a 3:1 ratio (Caco-2:HT29-MTX) were seeded onto the membranes at a concentration of 100,000 cells/cm^2. The cells were grown on the membrane for 16 days prior to experiments to allow for full coverage of the membrane and cell differentiation.

The systemic μCCAs were cleaned with 70% sulfuric acid and 30% hydrogen peroxide (30% H_2O_2 solution) for 10 min at room temperature and then rinsed with DI water. A 1-mm thick silicone gasket (Grace Bio-Labs, Bend, OR, gasket was cut to the correct size from a silicone sheet) with holes cut out over the corresponding cell chambers was placed onto the chips to keep coatings and cell suspensions

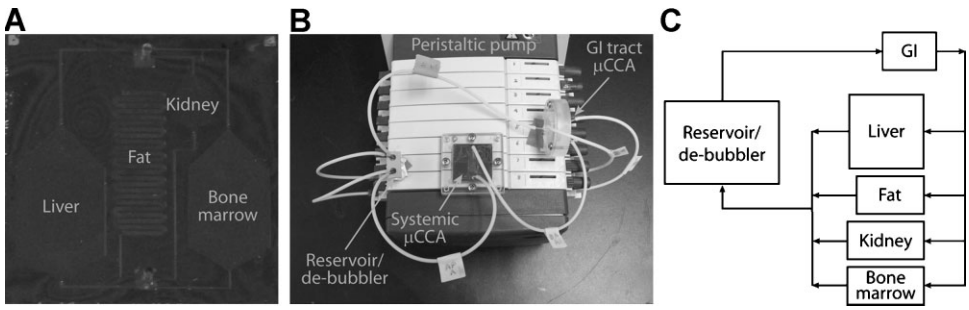

Figure 1. **(A)** Image of the systemic μCCA. The dimensions of the chambers are as follows ($w \times l \times d$): liver (8.5 mm × 8.25 mm × 30 μm), fat (0.5 mm × 115 mm × 100 μm), kidney (3.1 mm × 3.1 mm × 30 μm), and bone marrow (7.5 mm × 7.5 mm × 30 μm). The channels connecting compartments were 100 μm deep. The chip was designed so 41% of the flow went to the liver chamber, 35% went to the kidney chamber, 17% went to the bone marrow chamber, and 7% went to the fat chamber. The other poorly and well-perfused tissues were represented by the external de-bubbler, which was a 200 μL reservoir. **(B)** Image of the systemic and GI tract μCCA experimental set-up. **(C)** A schematic of the flow pattern in the μCCA system.

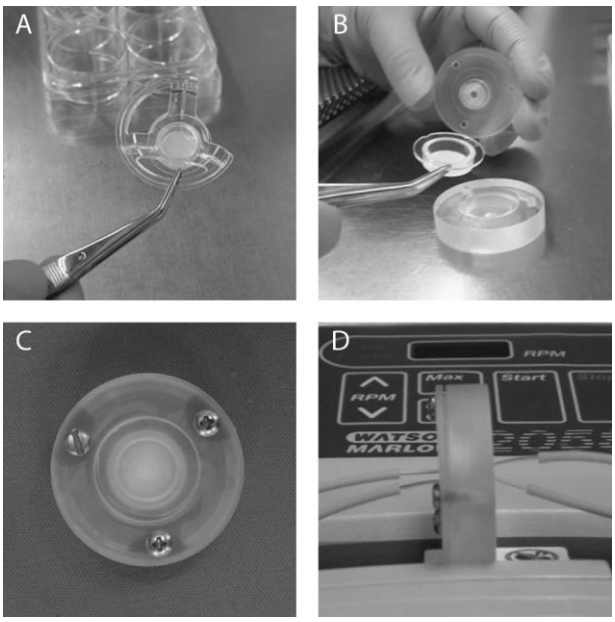

Figure 2. GI tract μCCA device and assembly. **(A)** The Snapwell membrane. **(B)** The Snapwell membrane being placed in between the top and bottom pieces of the GI tract μCCA. **(C)** The top of the assembled GI tract μCCA. **(D)** The inlets and outlets on the apical and basolateral sides of the assembled GI tract μCCA. The dimensions of the apical and basolateral chambers are as follows (diameter of the top of the chamber × height × diameter of the bottom of the chamber): apical chamber (0.8 mm × 0.8 mm × 2.8 mm) and basolateral chamber (2.8 mm × 0.8 mm × 0.8 mm). The total area of Caco-2/HT29-MTX cells exposed to flow was 6.2 mm^2.

within the proper compartments. The chips covered with gaskets were dried in an oven at 60°C for 30 min and autoclaved in a dry cycle for 30 min.

The systemic μCCAs were coated with 4 $\mu g/cm^2$ poly-D-lysine (Sigma–Aldrich, St. Louis, MO) for 5 min at room temperature. The poly-D-lysine solution was removed and each chamber was washed with an equal volume of PBS. The chips were next coated with 8 $\mu g/cm^2$ human plasma fibronectin (Millipore, Billerica, MA) for 1 h at room temperature. The fibronectin solution was removed, and HepG2/C3A cells were seeded into the liver chamber at a concentration of 250,000 cells/cm^2. The chips were kept at 37°C and 5% CO_2 for 4 h to allow the cells to attach and then the Petri dish holding the chips was filled with 25 mL of MEM. Cells were grown for 48 h before toxicity experiments.

Prior to toxicity experiments, autoclaved, 0.25 mm ID diameter, Pharmed peristaltic pump tubing (Cole-Parmer, Vernon Hills, IL) was placed into a peristaltic pump (Model 205S; Watson Marlow, Wilmington, MA) and MEM was pumped at 10 rpm through the tubing. Tips from 200 μL gel loading tips (Fisher Scientific, Hampton, NH), which fit securely into the inlet and outlet holes of the top and bottom pieces of the GI tract μCCA and plexiglass housing around the systemic μCCA, were inserted into the ends of the peristaltic pump tubing.

The GI tract μCCAs were assembled by placing a sterile silicone gasket into the bottom GI tract μCCA pieces. The gasket dimensions were 0.5 mm thick, 14 mm OD, and 4 mm ID (Grace Bio-Labs, gasket was cut to the correct size from a silicone sheet). Snapwell membranes were then detached from the insert that held them suspended in the six-well plates and the membranes were placed into the bottom chambers. A second sterile, silicone gasket (0.5 mm thick, 12 mm OD, and 4 mm ID) was placed inside the Snapwell membrane on top of the cell monolayer, and a third sterile, silicone gasket (1 mm thick, 14 mm ID, and 40 mm OD) was placed on the outer edge of the bottom GI tract μCCA piece. The top and bottom pieces were then screwed together tightly with the membrane holding Caco-2 and HT29-MTX cells in between them. The pump flow rate was decreased to 0.75 rpm, approximately 3.5 μL/min, and tubing from one pump channel was used for the GI tract μCCA apical or top inlet and tubing from a second pump channel was used for the basolateral or bottom inlet. Medium was pumped through the apical and basolateral GI tract μCCA chambers during chip assembly (~1 h) to rid the devices of air bubbles.

The silicone gaskets were peeled off the top of the systemic μCCAs and the chips were then placed between two pieces of 1/8 in. thick machined plexiglass that were screwed together tightly. The top pieces of plexiglass had two-step inlet and outlet holes (740 μm for the top half and 610 μm for the bottom half) and were cleaned with 70% EtOH and treated with oxygen plasma in an Expanded Plasma Cleaner (Harrick Plasma, Ithaca, NY) for 1 min before assembly to increase surface wettability and sterility (Chai et al., 2004). The bottom pieces of plexiglass were etched with ~1.5 mm deep squares that were slightly larger than the chips. A 1-mm thick piece of silicone gasket (Grace Bio-Labs) was placed into each of these cavities to allow for a tight seal between the top piece of plexiglass, chip, and bottom plexiglass piece. The bottom plexiglass piece was sterilized by soaking in 70% EtOH for 30 min prior to assembly. After removing the silicone gasket from the top of a chip, it was placed into the bottom plexiglass piece and 200 μL of MEM was pipetted on top of the chip. When pipetting MEM onto the chips, care was taken to remove any air bubbles in the liquid and to keep the liquid from spilling off of the chip and into the plexiglass chamber. The top plexiglass piece was then lowered straight down onto the chip, and the top and bottom pieces were screwed together.

After the systemic μCCAs were assembled, the outlet tubing from the basolateral side of the GI tract μCCA was connected to the inlet of the systemic μCCA and a separate tube was connected to the outlet after medium began to pool at the outlet hole. A 23-gauge, stainless steel needle was inserted into the tubing starts and ends. These needles were inserted into a well from an eight-well strip plate (Corning) sealed with a silicone cover (996050MR; BioTech Solutions, Mt. Laurel, NJ), which acted as a culture medium reservoir and de-bubbler. The basolateral side of the GI tract μCCA and systemic μCCA shared one reservoir that contained

200 μL of MEM. The apical side of the GI tract μCCA had a different reservoir that contained 250 μL of MEM (control) or MEM with 30, 10, 3, or 1 mM APAP.

The system was operated in an incubator at 37°C and 5% CO_2 for 24 h. At the end of the experiments, cells were stained with calcein (Invitrogen), a fluorescent viability stain, and monochlorobimane (MCB; Invitrogen), a fluorescent glutathione stain. MEM containing 5 μM calcein and 80 μM MCB was circulated through the GI tract and systemic μCCAs for 30 min at 37°C before imaging. Calcein was used in the Caco-2/HT29-MTX monolayers to visualize monolayer integrity, and results were discarded if the monolayers were damaged during assemble and did not remain intact.

In Vitro Digestion

Toxicity experiments were also performed after subjecting APAP to an in vitro digestion and using the chyme mimic as the drug transport solution. The in vitro digestion/Caco-2 cell culture model was developed by Glahn et al. (1998) for studying iron bioavailability from food. The compound of interest is subjected to an hour long pepsin digestion at 37°C and pH 2. The pepsin is then deactivated by raising the pH to 5.5–6.5 with sodium bicarbonate, a pancreatin-bile solution is added to the mixture, the pH is readjusted to 7.0 with sodium bicarbonate, and the chyme mimic is placed in an insert over a Caco-2 or Caco-2/HT29-MTX monolayer. In the in vitro digestion/APAP experiments, 30, 10, 3, and 1 mM APAP were digested and a control, drug-free digest was also prepared. A 250-μL aliquot was placed into a third reservoir and the chyme mimic was circulated through the apical GI chamber for 2 h. After 2 h the apical chamber tubing was moved to a reservoir containing MEM with no drug, and 22 h later cells were stained with calcein and MCB and imaged.

Fluorescence Microscopy and Image Analysis

Fluorescent images were acquired with a Retiga CCD camera (Qimaging, Burnaby, BC, Canada) mounted to an Olympus BX51 microscope (Olympus America, Inc., Center Valley, PA). The images were taken through a 10× objective in 12-bit grayscale format. Fluorescence from the calcein stain was collected with an EGFP cube (Ex 470/Em 610; Chroma Technology Corp., Rockingham, VT). Fluorescence from the MCB–glutathione adduct was collected with a DAPI cube (Ex 360/Em 460). Both image types (calcein, MCB–glutathione) were obtained in the same field of view. Six images were taken from each liver compartment and four images were taken of each Caco-2/HT29-MTX monolayer. Images were analyzed for total fluorescent area stained with Image Pro Plus version 4.6 software (Media Cybernetics, Inc., Silver Springs, MD).

Transepithelial Resistance Measurements

Transepithelial resistance (TER) of the cell monolayers in Snapwell inserts was measured every 3 days after seeding to assess the confluence of the monolayers and tight junction functionality. TER measurements were made using the Millicell ERS from Millipore with the Endohm-24 SNAP chamber from World Precision Instruments (Sarasota, FL). The chamber was sterilized prior to use with 70% ethanol for 15 min. After the chamber was equilibrated with 3 mL of PBS for 2 h at room temperature, the Millicell ERS voltage was adjusted to a zero reading and the PBS was replaced with 3 mL of serum-free DMEM. Culture plates were removed from the incubator 5 min prior to measurements to allow the culture medium to come to room temperature. Three measurements at different membrane insert positions were taken per sample. Membranes with TER values between 200 and 300 Ω/cm^2 were used for μCCA APAP toxicity experiments.

HPLC Analysis

APAP concentration in experimental culture medium was determined using the protocol described by Wang et al. (1996). Briefly, 100 μL of samples taken from the culture medium reservoirs were extracted with 50 μL acetonitrile and centrifuged at 3,000 rpm for 10 min. 2-Acetamindophenol was used as an internal standard. A 50-μL injection of the supernatant was used for determination of APAP and metabolites by reverse-phase HPLC analysis with a Waters 2690 separations module and Waters 996 photodiode array detector set at a wavelength of 254 nm (Waters Corporation, Milford, MA). Chromatogram analysis was performed using Millennium software (version 3.0; Waters). Separations were done on a 250 mm × 4.6 mm, 5 μm SUPELCOSIL™ ABZ-Plus column (Supelco, Bellefonte, PA). APAP was eluted with 7% acetonitrile (v/v, in water) with 0.1% trifluoroacetic acid (v/v) at a flow rate of 1.8 mL/min. Comparison with APAP, 2-acetamindophenol, APAP glucuronide (APAP-GLUC), or APAP sulfate (APAP-SULF) standards was used for APAP, internal standard, and metabolite identification and quantification.

Physiologically Based Pharmacokinetic Modeling

A PBPK model was developed for the distribution and metabolism of APAP in the human flow configuration (Fig. 3A) and the μCCA system flow configuration (Fig. 3B). The main purpose of this model was to aid in the development and design of the μCCA system by validating the flow pattern. The mathematical equations used were based on those described by El-Masri and Portier (1998). The organ or tissue volumes and blood flow rates used in the simulations were acquired from Brown et al. (1997), Davies and Morris (1993), and Kwon (2001). Partition coefficients were calculated using the method described by Poulin and

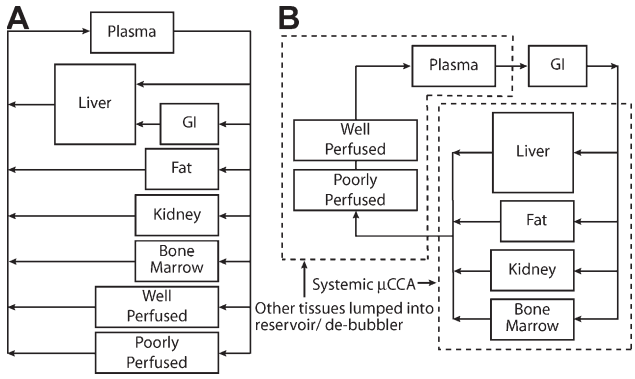

Figure 3. The physiologically correct, human blood flow pattern (**A**) and the medium flow pattern through the μCCA system (**B**).

Theil, and the metabolic parameters for conversion of APAP to NAPQI, APAP-GLUC, and APAP-SULF in the liver were obtained from Patten et al. (1993), Poulin and Theil (2002), and Watari et al. (1983). The absorption constant was calculated using the method described by Yu and Amidon assuming that 100% of the oral APAP dose is absorbed (Chiou and Barve, 1998; Yu and Amidon, 1999). The PBPK ordinary differential equations were solved with MATLAB version 7.1 (MathWorks, Natick, MA) using a fourth- and fifth-order Runge–Kutta–Fehlberg integration method.

Statistical Analysis

Results are expressed as mean ± standard error. Data were analyzed with GraphPad Prism version 4.00 for Windows (GraphPad Software, San Diego, CA). A one-way ANOVA with Tukey's post-test was used to compare differences between means, and data were transformed when necessary to obtain equal sample variances. Differences were considered significant at $P < 0.05$.

Results

Design of the μCCAs

Figure 1B is an image of the connected systemic and GI tract μCCAs, and Figure 1C is a schematic of the flow pattern in the μCCA system. Two channels were used on the peristaltic pump for the two devices. The first channel pumped MEM, MEM with APAP, chyme mimic, or chyme mimic with APAP through the apical chamber of the GI tract μCCA at ~3.5 μL/min. After the medium or chyme mimic passed through the apical chamber of the GI tract μCCA, it returned to a reservoir containing 250 μL of MEM, MEM with APAP, chyme mimic, or chyme mimic with APAP. The second channel pumped MEM at ~3.5 μL/min into the basolateral chamber of the GI tract μCCA and then to inlet or the silicon chip, mimicking systemic circulation. The flow immediately split after entering the systemic μCCA and 41% of the flow went to the liver chamber, 35% went to the kidney chamber, 17% went to the bone marrow chamber, and 7% went to the fat chamber. The culture medium from the chambers combined at the chip outlet and returned to a second reservoir containing 200 μL MEM before being re-circulated to the basolateral GI tract inlet. Figure 3 compares the physiologically correct, human blood flow pattern with the flow pattern through the systemic and GI tract μCCAs. The area under the curve (AUC), which corresponds to the total drug exposure, for the human configuration liver compartment was 92% of the μCCA configuration liver compartment AUC after 24 h according to PBPK results. This shows that in both configurations the liver should receive approximately the same APAP dose over a 24-h period. The systemic μCCA chambers and channels were designed so that the pressure drop was the same for each, allowing for a passive fluid flow split. The residence time was measured using the movement of an oil–water interface as described previously (Viravaidya et al., 2004). Table I compares the physiological parameter values for humans with those of the μCCA and the calculated μCCA chamber residence times with the measured residence times.

Table I. Comparison between human physiological parameter and μCCA design parameter values for the μCCA system.

	Human data			μCCA data			
	Body weight (% total)	Cardiac output (% total)	Residence time (min)	Compartment volume (% total)	Medium flow (% total)	Residence time (calculated) (min)	Residence time (measured) (min)
GI	2.4	19.6	1.5	1.0	100.0	0.6	0.6 ± 0.06
Liver	2.4	25.9	1.2	0.8	41.0	1.2	2.1 ± 0.3
Kidney	0.4	22.1	0.2	0.1	35.0	0.2	0.4 ± 0.1
Bone marrow	2.1	4.2	6.0	0.7	17.0	2.4	4.7 ± 0.8
Fat	14.3	4.6	38.5	4.5	7.0	38.5	30.3 ± 4.9
Other	78.4	16.8	48.1	92.8	100.0	55.7	

Values for human body weight, regional blood flow distribution, and organ residence times were taken from Brown et al. (1997) and Davies and Morris (1993). GI flow rates for the μCCA represent flow through the basolateral GI tract μCCA chamber. Values for measured residence times are expressed as mean ± SEM, $n = 3$.

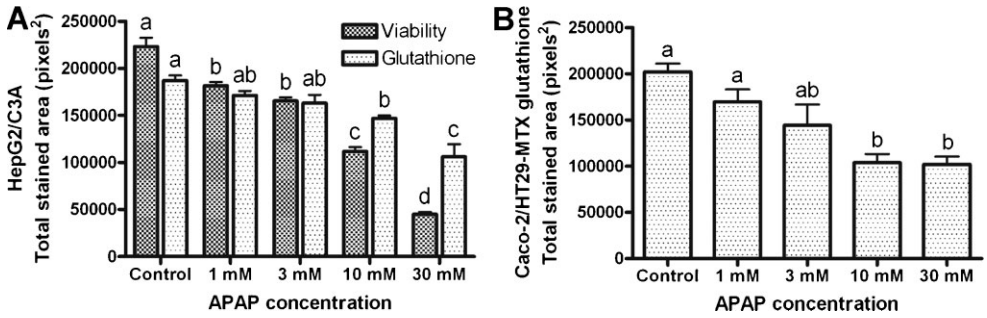

Figure 4. **A**: HepG2/C3A viability and glutathione levels and (**B**) Caco-2/HT29-MTX glutathione levels after culture medium with APAP was pumped through the apical chamber of the GI tract μCCA for 24 h. Controls had only culture medium pumped through the apical GI tract μCCA chamber. Values are expressed as mean ± SEM. Bars with no letter in common are significantly different according to a one-way ANOVA with Tukey's post-test ($P < 0.05$, $n = 3$).

μCCA Acetaminophen Toxicity

The results in Figure 4 show that as the concentration of APAP in the apical GI chamber increases, the viability and glutathione concentration of the cells in the liver compartment decrease. The glutathione levels also decreased with increasing APAP concentration in the Caco-2/HT29-MTX membranes (Fig. 4). Figures S1 and S2 in the supplementary information show representative fluorescent images of HepG2/C3A and Caco-2/HT20-MTX cells stained with calcein after a 24-h exposure to APAP absorbed through the GI tract μCCA apical chamber culture medium.

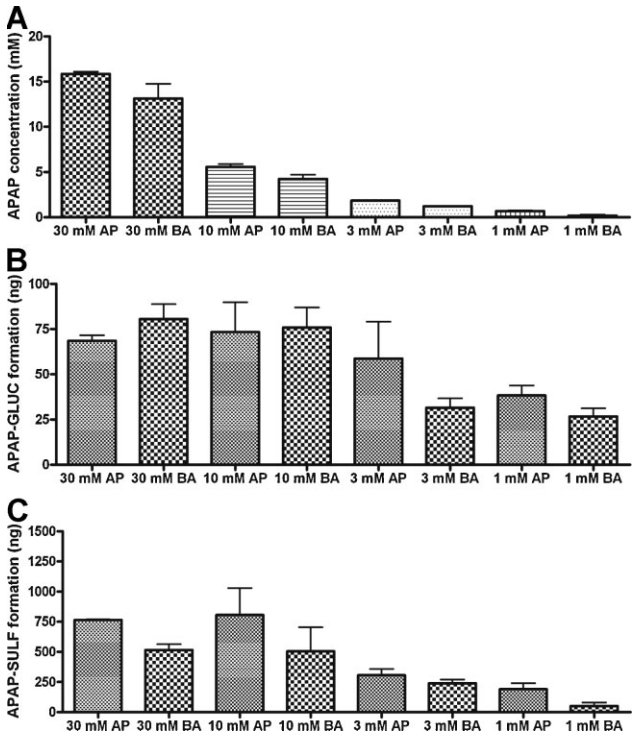

Figure 5. **A**: APAP, (**B**) APAP-GLUC, and (**C**) APAP-SULF concentration after 24 h in the apical GI reservoir (AP) and the basolateral GI/systemic reservoir (BA). Values are expressed as mean ± SEM, $n = 3$.

Figure 5 shows the APAP and APAP metabolite concentration after 24 h in the apical GI reservoir and the basolateral GI/chip reservoir. The APAP concentration was generally lower in the basolateral/chip reservoir, but this difference was not statistically significant for any of the doses. The formation of APAP-GLUC remained fairly constant for all APAP concentrations. This suggests that the UDP-glucuronyltransferase-catalyzed reaction was close to saturated levels even at low APAP exposure. The sulfotransferase activity was found to be much higher than UDP-glucuronyltransferase activity in these cell lines. The formation of APAP-SULF was approximately 10 times greater in the apical chamber with a 30 mM APAP dose when compared with APAP-GLUC. APAP-SULF formation generally decreased in the apical and basolateral chambers with decreasing APAP concentration, suggesting that at lower APAP concentrations this enzyme was not saturated.

A time-course experiment was performed with devices exposed to 10 mM APAP. The devices were disassembled at 2, 6, 12, and 24 h to determine APAP and metabolite concentration in the apical and basolateral chambers. These results are shown in Figure 6. The concentration of APAP in the basolateral/systemic reservoir gradually increased over the 24-h period, but never reached equilibrium with the apical chamber. The formation of APAP-GLUC reached saturation after 6 h in the basolateral chamber and chip. APAP-SULF formation increased over the 24-h period in the apical chamber and basolateral chamber/systemic circulation.

μCCA Digested Acetaminophen Toxicity

Figure 7 shows the results for experiments with digested APAP. As the APAP concentration in the apical chamber increased, the viability of liver cells and the glutathione levels of liver cells and Caco-2/HT29-MTX cells decreased significantly. The presence of digestive enzymes in the

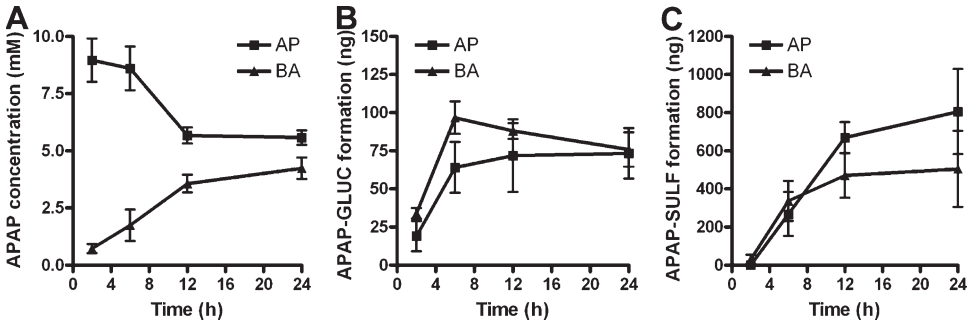

Figure 6. Results of HPLC analysis for a time-course experiment with devices exposed to 10 mM APAP. **A**: APAP, (**B**) APAP-GLUC, and (**C**) APAP-SULF concentrations at 2, 6, 12, and 24 h ($n=2$, $n=3$ for the 24-h time point).

chyme mimic did indirectly affect the viability of the liver cells, as the control viability for digestion experiments (Fig. 7) was approximately 25% lower than the control viability for experiments when only culture medium was circulated through the devices (Fig. 4).

Figure 8 shows the APAP and APAP metabolite concentration after a 2-h exposure to APAP in chyme mimic followed by culture medium with no drug for 22 h. The concentration of APAP in the apical and basolateral chambers was lower when compared with previous experiments where MEM containing APAP was circulated through the apical chamber for 24 h. When the chyme mimic containing 30 mM APAP was used, for example, the concentration of APAP in the apical chamber and basolateral chamber/chip reached ~3.5 mM after 24 h. There was no significant difference between the apical chamber and basolateral chamber/systemic circulation, which means that the APAP concentration reached equilibrium between the apical chamber and basolateral chamber/systemic circulation after 24 h for all concentrations tested. The formation of APAP-GLUC decreased for the lower APAP concentrations tested, which shows that at APAP concentrations lower than 1 mM, UDP-glucuronyltransferase is not saturated. APAP-SULF formation was much greater than APAP-GLUC formation, and APAP-SULF generally decreased in the apical chamber and basolateral chamber/systemic circulation with decreasing APAP concentration, which also indicates that at lower APAP concentrations the sulfotransferase pathway was not saturated.

Results from a time-course experiment with 10 mM digested APAP are shown in Figure 9. The devices were disassembled at 2, 6, 12, and 24 h to determine APAP and metabolite concentration in the apical and basolateral/systemic chambers. The concentration of APAP in the basolateral/systemic circulation reservoir reached equilibrium with the apical chamber by 6 h. The formation of APAP-GLUC was relatively low and approximately the same in the apical chamber and basolateral chamber/systemic circulation. APAP-SULF formation increased over the 24-h period in the apical chamber and basolateral chamber/systemic circulation at approximately the same rate. Although the total amount of APAP in the basolateral/systemic circulation reservoir was much lower when

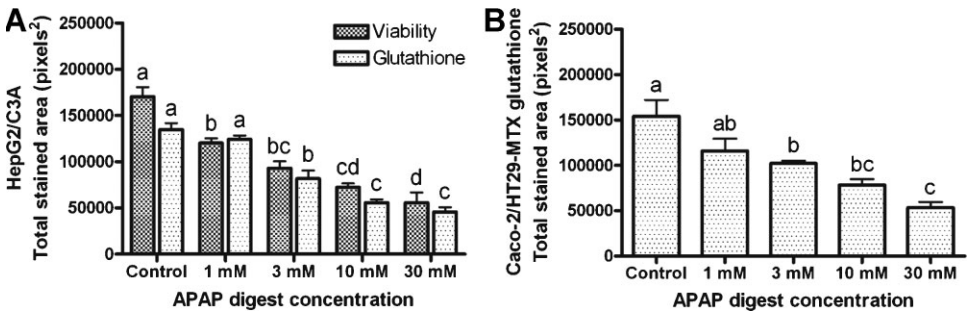

Figure 7. **A**: HepG2/C3A viability and glutathione levels and (**B**) Caco-2/HT29-MTX glutathione levels after APAP in chyme mimic was pumped through the apical chamber of the GI tract μCCA for 2 h followed by culture medium with no drug for 22 h. Controls had chyme mimic with no APAP circulated through the apical GI tract μCCA chamber for 2 h followed by culture medium with no drug for 22 h. Values are expressed as mean ± SEM. Bars with no letter in common are significantly different according to a one-way ANOVA with Tukey's post-test ($P<0.05$, $n=3$).

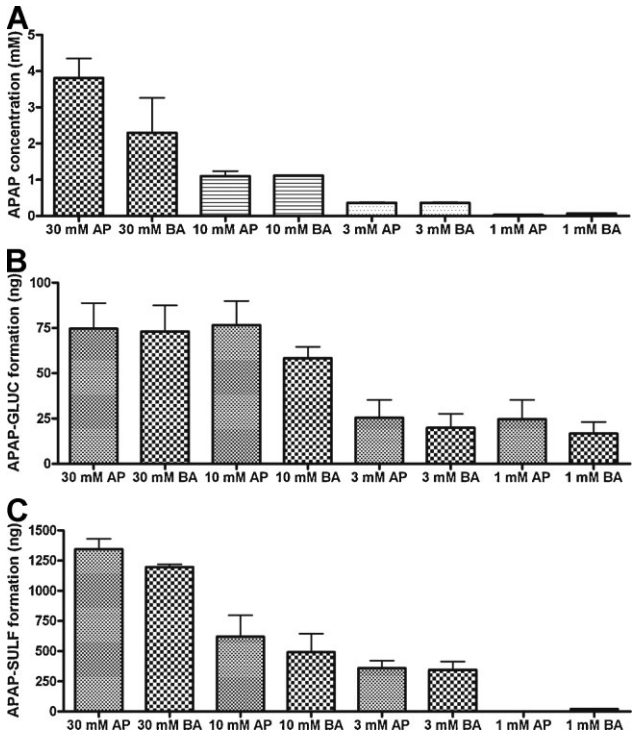

Figure 8. **A**: APAP, (**B**) APAP-GLUC, and (**C**) APAP-SULF concentration in the apical GI reservoir (AP) and the basolateral GI/systemic reservoir (BA) after APAP in chyme mimic was pumped through the apical chamber of the GI tract μCCA for 2 h followed by culture medium with no drug for 22 h. Values are expressed as mean ± SEM, $n = 3$.

compared with the experiments when APAP was delivered in MEM (~5 mM in the basolateral/systemic circulation reservoir for experiments with APAP in MEM and ~1 mM in the basolateral/systemic circulation reservoir for experiments with digested APAP), the amount of APAP-GLUC and APAP-SULF formed was similar between the two experiments.

APAP was not soluble in the culture medium or chyme mimic at the desired concentrations, so it was dissolved in 95% ethanol before dilution in MEM or digestion. At high concentrations of APAP, this resulted in a considerable amount (5.7% at 30 mM and 1.9% at 10 mM) of ethanol in the culture medium. Control experiments were performed to determine the effects of ethanol on HepG2/C3A cell viability and glutathione levels and GI cell glutathione levels, and these results are shown in the supplemental information in Figure S3. It was found that there was statistically significant cell death caused by 5.7% (v/v) ethanol in culture medium (approximately 17% cell death), but HepG2/C3A cells exposed to 1.9% ethanol in culture medium were not significantly affected after 24-h experiments.

Discussion

APAP is a weak organic acid ($pK_a = 9.7$) that is non-ionized at pH 7 (Rang et al., 1999). Because APAP is a small molecule and non-ionized at a physiological pH, it is able to passively diffuse through the small intestinal cell membrane. Passive diffusion of a drug involves the movement of drug molecules down a concentration gradient without the expenditure of energy and the rate of penetration of a drug across a membrane is related to the concentration gradient by Fick's law (Rang et al., 1999). APAP is one of the most widely used analgesic and antipyretic drugs by children and adults worldwide, and the pharmacological side effects are thought to be based on the inhibition of prostaglandin synthesis (Bessems and Vermeulen, 2001; Kociancic and Reed, 2003). Therapeutic doses of immediate release APAP preparations are normally absorbed from the GI tract within 1 h, while peak serum concentrations in acute overdose may be delayed for up to 4 h (Kociancic and Reed, 2003). A common tool that is used to predict potential hepatotoxic APAP effects is the Rumack–Matthew scale (1975). The nomogram has a line from 200 mg/L serum APAP concentration at 4 h to 50 mg/L at 12 h after APAP overdose. Untreated patients with a serum APAP concentration above

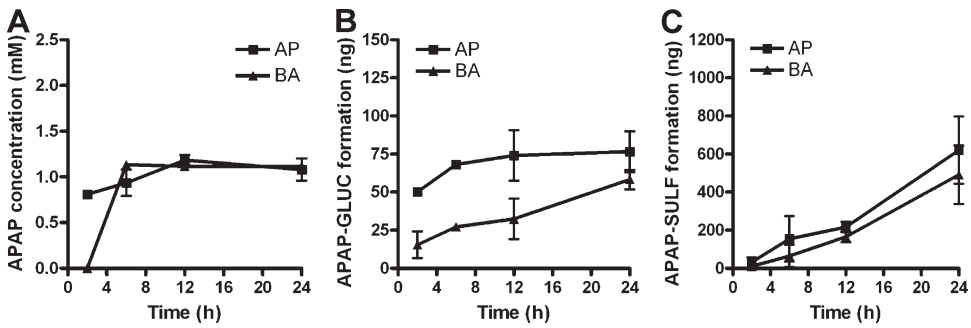

Figure 9. Results of HPLC analysis for a time-course experiment with devices exposed to 10 mM APAP in chyme mimic for 2 h followed by culture medium with no drug for 22 h. **A**: APAP, (**B**) APAP-GLUC, and (**C**) APAP-SULF concentration at 2, 6, 12, and 24 h ($n = 2$, $n = 3$ for the 24-h time point).

the line are considered at risk for hepatic damage. The liver toxicity is due to CYP bioactivation of APAP to a reactive metabolite, NAPQI (Patten et al., 1993). A 200 mg/L serum concentration is approximately 1 mM, which was the lowest APAP concentration tested with the μCCA devices.

We previously described a prototype in vitro system that for the first time, although at a very basic level, mimicked oral exposure to a drug, first pass metabolism, and the circulation of metabolites on a microscale (McAuliffe et al., 2008). These results demonstrated that APAP could cross the Caco-2 cell monolayer and damage cells in the liver and lung compartments (McAuliffe et al., 2008). In these previously published experiments, APAP was significantly more toxic to the liver cells when APAP was delivered directly to the systemic circulation (mimicking intravenous infusion) rather than absorbed through the GI tract μCCA. When the first-generation GI tract μCCA was included in the experiments, APAP was absorbed slowly into the systemic μCCA circulation. Further, metabolism by the GI cells reduced the APAP load on the liver cells. The first-generation chip and GI tract μCCAs provided a framework for studying oral drug absorption and metabolism, but the first-generation system had several limitations. These problems led to the development of the second-generation μCCA system described here (Figs. 1 and 2). The second-generation systemic μCCA was designed with only one inlet and outlet to reduce the amount of air that enters the system, which allowed for longer operation and use of more physiologically realistic APAP concentrations. Goblet-like, mucus-secreting cells were incorporated into the second-generation GI tract μCCA membrane to better mimic the cell composition in vivo. HPLC was used to determine the APAP and metabolite concentrations at different time points throughout the experiment. Finally, in vitro digestion of APAP was performed and this chyme mimic was pumped through the apical chamber of the second-generation GI tract, which better recreates the absorption conditions in the upper small intestine. These changes make the second-generation system more physiologically accurate.

The results generated using the second-generation GI tract and systemic μCCAs demonstrate that liver and intestinal epithelial cells in the chip and GI tract μCCAs respond to APAP in a dose-dependent manner for APAP in culture medium or chyme mimic (Figs. 4 and 7). As the concentration of APAP in culture medium or chyme mimic circulated through the apical chamber of the GI tract μCCA increased the viability of the liver cells and the glutathione levels of the liver and intestinal epithelial cells decreased. Some decrease in cell viability was due to ethanol, the APAP solvent, for the 30 mM concentration (Fig. S3). The 30 mM dose was used to provide a comparison to in vivo data, but the inhibitory level of ethanol makes this high dose less useful. MCB was the fluorescent glutathione stain used, and glutathione levels in the μCCA system did not decrease as significantly as viability levels. There was a great deal of background after staining the cells with MCB and this background is why the glutathione levels do not appear to decrease as rapidly as viability. In the future, staining for glutathione in human cells with this system may be improved by using monobromobimane (Hedley and Chow, 1994).

APAP metabolism to APAP-GLUC and APAP-SULF was higher in the digested samples when compared with the non-digested samples (Figs. 5 and 8), which could be due to the method of delivery of APAP to the systemic μCCA in the digestion experiments. APAP was delivered for 2 h in the digestion experiments and then followed with fresh culture medium for 22 h. This may have allowed the cells to better metabolize APAP when compared with a constant infusion of APAP over 24 h. Overall, APAP-SULF and APAP-GLUC were formed in the ng range, while the system was exposed to APAP in the mg range. Although this system is mimicking overdose conditions, in which the amount of APAP in the system overwhelms the ability of the liver to metabolize the drug, the metabolizing enzyme activity of the cell lines is also lower than that found in vivo. Future experiments to increase the metabolizing enzyme activity include the possible use of primary cells and the encapsulation of cells in a gel or matrix to form a 3D structure that is more organ or tissue-like.

When APAP was circulated through the apical GI μCCA chamber in MEM for 24 h, the concentrations of APAP in the apical chamber and basolateral chamber/systemic circulation reached near equilibrium after 24 h for all of the concentrations (Fig. 5). The time-course experiment with 10 mM APAP showed that the APAP concentrations in the two chambers did not reach equilibrium until after the 12-h time point (Fig. 6). In this system, absorption of APAP most likely occurs via passive diffusion down a concentration gradient; therefore, complete absorption would mean that the concentration in the apical chamber and basolateral chamber/chip is equal. In vivo, APAP is completely absorbed within 1 h at therapeutic doses. Peak serum concentrations in acute overdose, however, may be delayed for up to 4 h, which means that complete absorption would be expected within 5 h (Kociancic and Reed, 2003). Passively diffused drugs diffuse through the intestinal epithelium at a constant rate, and the transport of passively diffused drugs through Caco-2 monolayers has been shown to correlate well with in vivo data (Lennernas et al., 1996). Therefore, one likely reason that APAP takes two to three times longer to reach equilibrium in the μCCA is the lower amount of surface area available for absorption in the device when compared with the small intestine in vivo. In future work, the surface area available for absorption could easily be increased in the devices.

When APAP was circulated through the apical GI chamber in chyme mimic, the APAP concentration in the apical chamber and basolateral chamber/chip reached near equilibrium after 24 h for all concentrations studied (Fig. 8). The time-course experiment with 10 mM APAP showed that the APAP concentrations in the two chambers reached

equilibrium by approximately 6 h (Fig. 9). An explanation for why the system reached equilibrium more quickly when digested APAP was used may be that the chyme mimic slightly damaged the Caco-2/HT29-MTX monolayer. This may have compromised the tight junctions and resulted in more drug passing through the epithelial layer. Ingels et al. (2002) have shown that simulated intestinal buffers are compatible with Caco-2 monolayers for up to 2 h, but cause a ~25% decrease in TER value.

An important consideration when developing a μCCA is the comparison with in vivo data. A mouse has 74.5 mL blood/kg, so a 0.02 kg mouse has about 1.5 mL of blood (Kwon, 2001). A 300 mg/kg APAP dose to a 0.02 kg mouse (with 100% absorption) would therefore result in a systemic APAP concentration of about 27 mM. Mice given a 300 mg/kg dose of APAP had $67 \pm 12\%$ necrotic liver cells after 24 h (Gujral et al., 2002). In the μCCA system exposed to 30 mM APAP in culture medium, there was about $80 \pm 3\%$ cell death, and in the μCCA system exposed to 30 mM digested APAP, there was $67 \pm 16\%$ cell death. Both of these results are within the range of the mouse in vivo results, although synergistic effects between the ethanol used as a carrier and APAP on cell viability at the 30 mM concentration may have occurred.

In conclusion, a GI tract μCCA has been developed and used together with a systemic μCCA to demonstrate absorption, distribution, metabolism, and toxicity of APAP. Our results indicate that APAP was absorbed and metabolized by GI cells, resulting in GI cell glutathione depletion. APAP then circulated to the liver compartment, where it was further metabolized by liver cells into a reactive metabolite that caused liver cell glutathione depletion and toxicity in a dose-dependent manner that agrees with in vivo results.

The μCCA system can overcome many of the drawbacks found in traditional drug testing methods. Multiple cell types and re-circulating medium allow researchers to analyze the absorption and the systemic effects of the compound being studied and the effects of its metabolites in a way that mimics the dynamic, time-dependent changes in drug concentration and metabolites after oral administration. Human cells can be used in the μCCAs, offering a superior method for predicting a potential drug's effect on humans and sparing animals. The μCCAs are also inexpensive to produce and use very little of the compound of interest. The development and incorporation of a physiologically realistic GI tract μCCA provide a new tool to help predict the systemic toxicity of orally delivered drugs or ingested chemicals.

Financial support for this work was provided by the Nanobiotechnology Center (NBTC), an STC Program of the National Science Foundation, under Agreement No. ECS-9876771; the New York State Office of Science, Technology and Academic Research (NYSTAR) program through a grant to MLS as a NYSTAR Distinguished Professor; the Army Corps of Engineers under Agreement ID W9132T-07-2-0010; and the U.S. Department of Agriculture via the collaboration with RPG. This work was performed in part at the Cornell NanoScale Facility, a member of the National Nanotechnology Infrastructure Network, which is supported by the National Science Foundation (Grant ECS-0335765). The HT29-MTX cell line was kindly contributed by Dr. Thécla Lesuffleur of INSERM U560 in Lille, France.

References

Agres T. 2005. Finding blockbusters a struggle. Drug Discov Dev 8(3):16–19.

Artursson P, Karlsson J. 1991. Correlation between oral drug absorption in humans and apparent drug permeability coefficients in human intestinal epithelial (Caco-2) cells. Biochem Biophys Res Commun 175(3): 880–885.

Artursson P, Palm K, Luthman K. 2001. Caco-2 monolayers in experimental and theoretical predictions of drug transport. Adv Drug Deliver Rev 46(1–3):27–43.

Atuma C, Strugala V, Allen A, Holm L. 2001. The adherent gastrointestinal mucus gel layer: Thickness and physical state in vivo. Am J Physiol Gastrointest Liver Physiol 280(5):G922–G929.

Audus KL, Bartel RL, Hidalgo IJ, Borchardt RT. 1990. The use of cultured epithelial cells for drug transport and metabolism studies. Pharm Res 7(5):435–451.

Baranczykkuzma A, Garren JA, Hidalgo IJ, Borchardt RT. 1991. Substrate-specificity and some properties of phenol sulfotransferase from human intestinal Caco-2 cells. Life Sci 49(16):1197–1206.

Bessems JGM, Vermeulen NPE. 2001. Paracetamol (acetaminophen)-induced toxicity: Molecular and biochemical mechanisms, analogues and protective approaches. Crit Rev Toxicol 31(1):55–138.

Borlak J, Zwadlo C. 2003. Expression of drug-metabolizing enzymes, nuclear transcription factors, and ABC transporters in Caco-2 cells. Xenobiotica 33(9):927–943.

Brand RM, Hannah TL, Mueller C, Cetin Y, Hamel FG. 2000. A novel system to study the impact of epithelial barriers on cellular metabolism. Ann Biomed Eng 28(10):1210–1217.

Brown RP, Delp MD, Lindstedt SL, Rhomberg LR, Beliles RP. 1997. Physiological parameter values for physiologically based pharmacokinetic models. Toxicol Ind Health 13(4):407–484.

Chai JN, Lu FZ, Li BM, Kwok DY. 2004. Wettability interpretation of oxygen plasma modified poly(methyl methacrylate). Langmuir 20(25): 10919–10927.

Chiou WL, Barve A. 1998. Linear correlation of the fraction of oral dose absorbed of 64 drugs between humans and rats. Pharm Res 15(11): 1792.

Choi SH, Fukuda O, Sakoda A, Sakai Y. 2004a. Enhanced cytochrome P450 capacities of Caco-2 and HepG2 cells in new coculture system under the static and perfused conditions: Evidence for possible organ-to-organ interactions against exogenous stimuli. Mat Sci Eng C 24(3):333.

Choi SH, Nishikawa M, Sakoda A, Sakai Y. 2004b. Feasibility of a simple double-layered coculture system incorporating metabolic processes of the intestine and liver tissue: Application to the analysis of benzo[a]pyrene toxicity. Toxicol In Vitro 18(3):393–402.

Corcoran GB, Mitchell JR, Vaishnav YN, Horning EC. 1980. Evidence that acetaminophen and n-hydroxyacetaminophen form a common arylating intermediate, n-acetyl-para-benzoquinoneimine. Mol Pharmacol 18(3):536–542.

Davies B, Morris T. 1993. Physiological parameters in laboratory animals and humans. Pharm Res 10(7):1093.

Doherty MM, Charman WN. 2002. The mucosa of the small intestine: How clinically relevant as an organ of drug metabolism? Clin Pharmacokinet 41(4):235–253.

El-Masri HA, Portier CJ. 1998. Physiologically based pharmacokinetics model of primidone and its metabolites phenobarbital and phenylethylmalonamide in humans, rats, and mice. Drug Metab Dispos 26(6):585–594.

Forstner JF, Forstner GG. 1994. Gastrointestinal mucus. In: Johnson LR, editor. Physiology of the gastrointestinal tract. 3rd edn. New York: Raven Press, p 1255–1283.

Glahn RP, Lee OA, Yeung A, Goldman MI, Miller DD. 1998. Caco-2 cell ferritin formation predicts nonradiolabeled food iron availability in an in vitro digestion/Caco-2 cell culture model. J Nutr 128:1555–1561.

Gujral JS, Knight TR, Farhood A, Bajt ML, Jaeschke H. 2002. Mode of cell death after acetaminophen overdose in mice: Apoptosis or oncotic necrosis? Toxicol Sci 67(2):322–328.

Hedley DW, Chow S. 1994. Evaluation of methods for measuring cellular glutathione content using flow cytometry. Cytometry 15(4):349–358.

Hewitt NJ, Hewitt P. 2004. Phase I and II enzyme characterization of two sources of HepG2 cell lines. Xenobiotica 34(3):243–256.

Hilgendorf C, Spahn-Langguth H, Regardh CG, Lipka E, Amidon GL, Langguth P. 2000. Caco-2 versus Caco-2/HT29-MTX co-cultured cell lines: Permeabilities via diffusion, inside- and outside-directed carrier-mediated transport. J Pharm Sci 89(1):63–75.

Ingels F, Deferme S, Destexhe E, Oth M, Van den Mooter G, Augustijns P. 2002. Simulated intestinal fluid as transport medium in the Caco-2 cell culture model. Int J Pharm 232(1–2):183.

Kociancic T, Reed MD. 2003. Acetaminophen intoxication and length of treatment: How long is long enough? Pharmacotherapy 23(8):1052–1059.

Kwon Y. 2001. Handbook of essential pharmacokinetics, pharmacodynamics and drug metabolism for industrial scientists. New York: Kluwer Academic, p 230–231.

Lampen A, Bader A, Bestmann T, Winkler M, Witte L, Borlak JT. 1998. Catalytic activities, protein- and mRNA-expression of cytochrome P450 isoenzymes in intestinal cell lines. Xenobiotica 28(5):429–441.

Lau YY, Chen YH, Liu TT, Li C, Cui XM, White RE, Cheng KC. 2004. Evaluation of a novel in vitro Caco-2 hepatocyte hybrid system for predicting in vivo oral bioavailability. Drug Metab Dispos 32(9):937–942.

Lee HJ. 2002. Protein drug oral delivery: The recent progress. Arch Pharm Res 25(5):572–584.

Lennernas H, Palm K, Fagerholm U, Artursson P. 1996. Comparison between active and passive drug transport in human intestinal epithelial (Caco-2) cells in vitro and human jejunum in vivo. Int J Pharm 127: 103–107.

Lesuffleur T, Barbat A, Dussaulx E, Zweibaum A. 1990. Growth adaptation to methotrexate of HT-29 human colon-carcinoma cells is associated with their ability to differentiate into columnar absorptive and mucus-secreting cells. Cancer Res 50(19):6334–6343.

Mahler GJ, Shuler ML, Glahn RP. 2008. Characterization of Caco-2 and HT29-MTX cocultures in an in vitro digestion/cell culture model used to predict iron bioavailability. J Nutr Biochem. DOI: 10.1016/j.jnutbio.2008.05.006.

McAuliffe GJ, Chang JY, Glahn RP, Shuler ML. 2008. Development of a gastrointestinal tract microscale cell culture analog to predict drug transport. Mol Cell Biomech 5(2):119–132.

Mitchell JR, Jollow DJ, Potter WZ, Gillette JR, Brodie BB. 1973. Acetaminophen-induced hepatic necrosis. 4. Protective role of glutathione. J Pharmacol Exp Ther 187(1):211–217.

Newton JL, Jordan N, Pearson J, Williams GV, Allen A, James OFW. 2000. The adherent gastric antral and duodenal mucus gel layer thins with advancing age in subjects infected with helicobacter pylori. Gerontology 46(3):153–157.

Patten CJ, Thomas PE, Guy RL, Lee MJ, Gonzalez FJ, Guengerich FP, Yang CS. 1993. Cytochrome-P450 enzymes involved in acetaminophen activation by rat and human liver-microsomes and their kinetics. Chem Res Toxicol 6(4):511–518.

Poulin P, Theil FP. 2002. Prediction of pharmacokinetics prior to in vivo studies. 1. Mechanism-based prediction of volume of distribution. J Pharm Sci 91(1):129–156.

Prueksaritanont T, Gorham LM, Hochman JH, Tran LO, Vyas KP. 1996. Comparative studies of drug-metabolizing enzymes in dog, monkey, and human small intestine cells, and in Caco-2 cells. Drug Metab Dispos 24(6):634–642.

Qiu YC, Benet LZ, Burlingame AL. 1998. Identification of the hepatic protein targets of reactive metabolites of acetaminophen in vivo in mice using two-dimensional gel electrophoresis and mass spectrometry. J Biol Chem 273(28):17940–17953.

Rang HP, Dale MM, Ritter JM. 1999. Pharmacology. 4th edn. Edinburgh: Churchill Livingston.

Rumack BH, Matthew H. 1975. Acetaminophen poisoning and toxicity. Pediatrics 55(6):871–876.

Sankar U. 2005. The delicate toxicity balance in drug discovery. Scientist 19(15):32–34.

Sin A, Chin KC, Jamil MF, Kostov Y, Rao G, Shuler ML. 2004. The design and fabrication of three-chamber microscale cell culture analog devices with integrated dissolved oxygen sensors. Biotechnol Progr 20(1):338–345.

Tatosian DA, Shuler ML. 2009. A novel system for evaluation of drug mixtures for potential efficacy in treating multidrug resistant cancers. Biotechnol Bioeng 103(1):187–198.

Viravaidya K, Shuler ML. 2004. Incorporation of 3T3-L1 cells to mimic bioaccumulation in a microscale cell culture analog device for toxicity studies. Biotechnol Progr 20(2):590–597.

Viravaidya K, Sin A, Shuler ML. 2004. Development of a microscale cell culture analog to probe naphthalene toxicity. Biotechnol Progr 20(1): 316–323.

Walter E, Janich S, Roessler BJ, Hilfinger JM, Amidon GL. 1996. HT29-MTX/Caco-2 cocultures as an in vitro model for the intestinal epithelium: In vitro in vivo correlation with permeability data from rats and humans. J Pharm Sci 85(10):1070–1076.

Wang EJ, Li Y, Lin M, Chen LS, Stein AP, Reuhl KR, Yang CS. 1996. Protective effects of garlic and related organosulfur compounds on acetaminophen-induced hepatotoxicity in mice. Toxicol Appl Pharm 136(1):146–154.

Watari N, Iwai M, Kaneniwa N. 1983. Pharmacokinetic study of the fate of acetaminophen and its conjugates in rats. J Pharmacokinet Biopharm 11(3):245–272.

Wikman A, Karlsson J, Carlstedt I, Artursson P. 1993. A drug absorption-model based on the mucus layer producing human intestinal goblet cell-line HT29-H. Pharm Res 10(6):843–852.

Yu LX, Amidon GL. 1999. A compartmental absorption and transit model for estimating oral drug absorption. Int J Pharm 186(2):119.